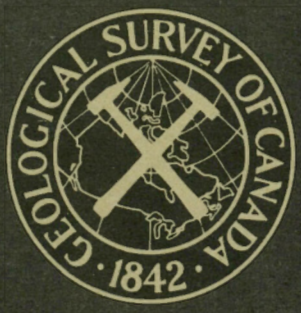

GEOLOGICAL
SURVEY
OF
CANADA

DEPARTMENT OF MINES
AND TECHNICAL SURVEYS

PAPER 64-43

THE DESIGN OF A SPINNER-TYPE REMANENT MAGNETOMETER

Report and 10 figures

A. Larochelle

Price 35 cents

1965

GEOLOGICAL SURVEY

OF CANADA

PAPER 64-43

THE DESIGN OF A SPINNER-TY REMANENT MAGNETOMETER

A. Larochelle

DEPARTMENT OF MINES AND TECHNICAL SURVEYS

Available by mail from the Queen's Printer, Ottawa,
from Geological Survey of Canada,
601 Booth St., Ottawa,
and at the following Canadian Government bookshops:

OTTAWA
Daly Building, corner Mackenzie and Rideau

TORONTO
Mackenzie Building, 36 Adelaide St. East

MONTREAL
Æterna-Vie Building, 1182 St. Catherine St. West

or through your bookseller

A deposit copy of this publication is also available
for reference in public libraries across Canada

Price 75 cents Cat. No. M44-64/43

Price subject to change without notice

ROGER DUHAMEL, F.R.S.C.
Queen's Printer and Controller of Stationery
Ottawa, Canada
1965

CONTENTS

Page

Abstract v
Introduction 1
Acknowledgments 1
Theory of the spinner remanent magnetometer 2
Design of the Geological Survey's instrument 11
Conclusions 22
Bibliography 22

Table I. Sample volumes and spinning frequencies reported in the literature 12

Illustrations

Plate I. The Geological Survey's spinner magnetometer vi

Figure 1. Geometric configuration of pick-up coil and measured dipole 3
2. Equivalent circuit of matching transformer 3
3. Theoretical variation of F(m,n,p) 8
4. Details of air turbine 13
5. Turbine-coil configurations 15
6. Longitudinal cross-section of coil system 16
7. Block diagram of electronic circuitry 18
8. Calibration curves of the spinner magnetometer 20
9. Variation of $\log_{10}(25\alpha + 6)\mu_c$ vs. β 21
10. Circuit diagram ..... in pocket

ABSTRACT

The theory of the spinner remanent magnetometer is reviewed and a description is given of an instrument of this type that was developed recently at the Geological Survey of Canada. With this instrument, 1-inch rock cubes are spun at the rate of 255 cycles per second by means of a conical air turbine located at the centre of a solenoidal pick-up coil. The instrument's maximum sensitivity, about 2.2×10^{-6} cgs units per cc, allows measuring the natural remanent magnetization of most volcanic rocks and some red beds.

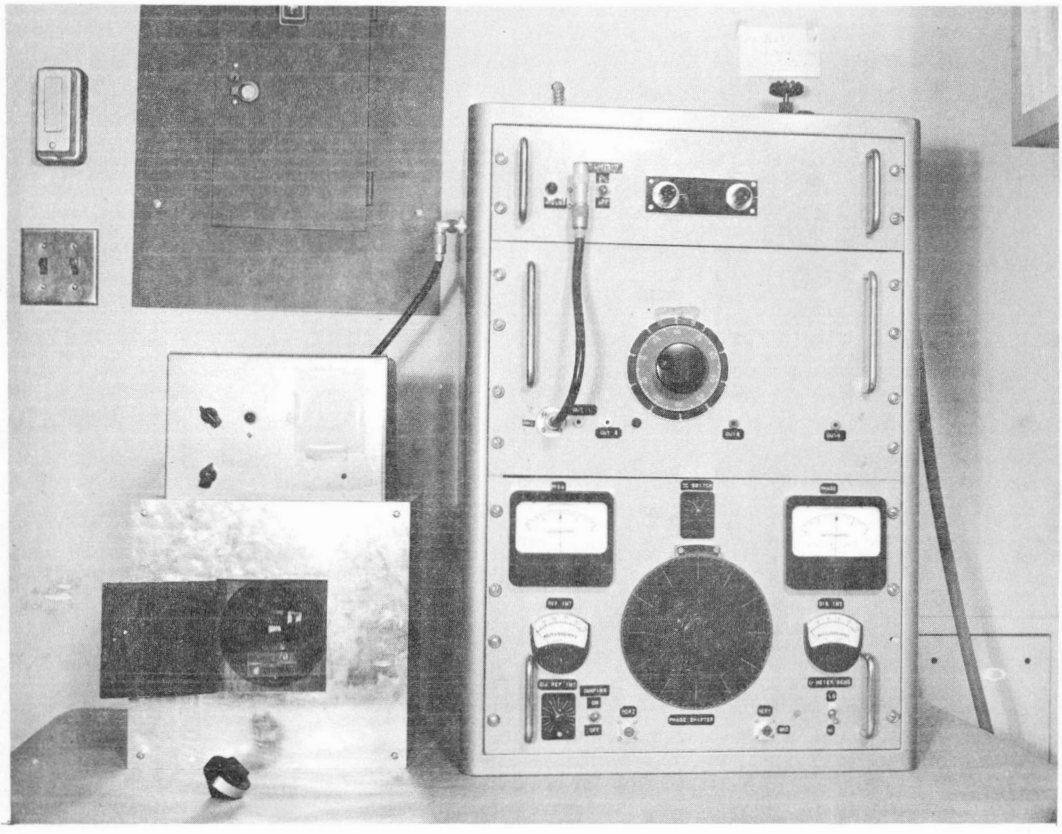

Plate I. The Geological Survey's spinner magnetometer.

THE DESIGN OF A SPINNER-TYPE REMANENT MAGNETOMETER

INTRODUCTION

With the increasing number of laboratories engaged in palaeomagnetic research, many instruments have been proposed for measuring the N.R.M. (natural remanent magnetization) of rocks. Most of these instruments belong to either the "spinner" type or the "astatic" type. Whereas most astatic magnetometers described so far in the literature depart only slightly if at all from the classic design of Blackett (1952)[1], many differences exist among the various spinner magnetometers built since the early publication of a paper by McNish and Johnson (1938) on the design of such an instrument.

In principle a spinner-type magnetometer is an A.C. generator in which the rotating magnetic field is produced by the spinning of a permanently magnetized body near a fixed pick-up coil. The intensity of the emf induced in the coil is proportional to the rate of spinning and to the component of the sample's remanent magnetization in the plane perpendicular to the spinning axis. If the sample consists of a small body of rock (as in the case of palaeomagnetic measurements), the emf will generally be very small and will have to be amplified several thousands of times if its intensity is to be measured accurately. Hence it is necessary to have a high-gain amplifier among other electronic components in the make-up of a spinner-type magnetometer.

Acknowledgments

The writer acknowledges the work of H.W.C. Knapp, R.H. Ahrens, and C. Gauvreau, who adapted a circuit diagram to the instrument. The circuit diagram was kindly supplied to the writer by the Carnegie Institute in Washington. The machining of the turbine was done by A.G. Meilleur; D. McClure carried out the calibration measurements.

[1]Names and/or dates in parenthesis refer to publications listed in the Bibliography.

THEORY OF THE SPINNER REMANENT MAGNETOMETER

Let us assume a magnetic dipole, μ, whose components μ_x, μ_y and μ_z are oriented respectively along the axes x, y, and z of a rectangular system of coordinates whose origin coincides with the centre of the dipole (Fig. 1). We may express the magnetic potential due to this dipole at a point P(x, y, z) as

$$W_p = \frac{\mu_x x + \mu_y y + \mu_z z}{R^3} \quad \ldots\ldots\ldots\ldots\ldots\ldots\ldots\ldots\ldots\ldots (1)$$

where $R = \sqrt{x^2 + y^2 + z^2} = \sqrt{r^2 + z^2}$

Assuming now that P is any point on a circular loop perpendicular to and centred on, say, the z axis, the z component of the dipole field H_z at P is given by

$$H_z = \frac{-\partial W_p}{\partial Z} = \frac{-\mu_z (r^2 - 2z^2) + 3rz\, \mu_x \cos(\alpha - \theta) \Big/ \cos\alpha}{R^5} \quad \ldots (2)$$

where $\tan\alpha = \mu_y/\mu_x$ and $\tan\theta = y/x$.

By virtue of symmetry, the contributions of μ_x to H_z at P and to H_z' at P', diametrically opposed to P, are equal and of opposite signs. Thus, upon integrating the magnetic flux, ϕ, over the area bounded by the loop, the cosine term in equation (2) cancels out and it follows that

$$\phi = \int_0^{2\pi} \left[\int_0^r \frac{\mu_z (r^2 - 2z^2)\, r\,dr}{R^5} \right] d\theta = \frac{2\pi \mu_z r^2}{(r^2 + z^2)^{3/2}} \quad \ldots\ldots\ldots (3)$$

Replacing the single loop by a large number of turns, as represented by the circular coil whose section appears in Figure 1, the flux linkage becomes

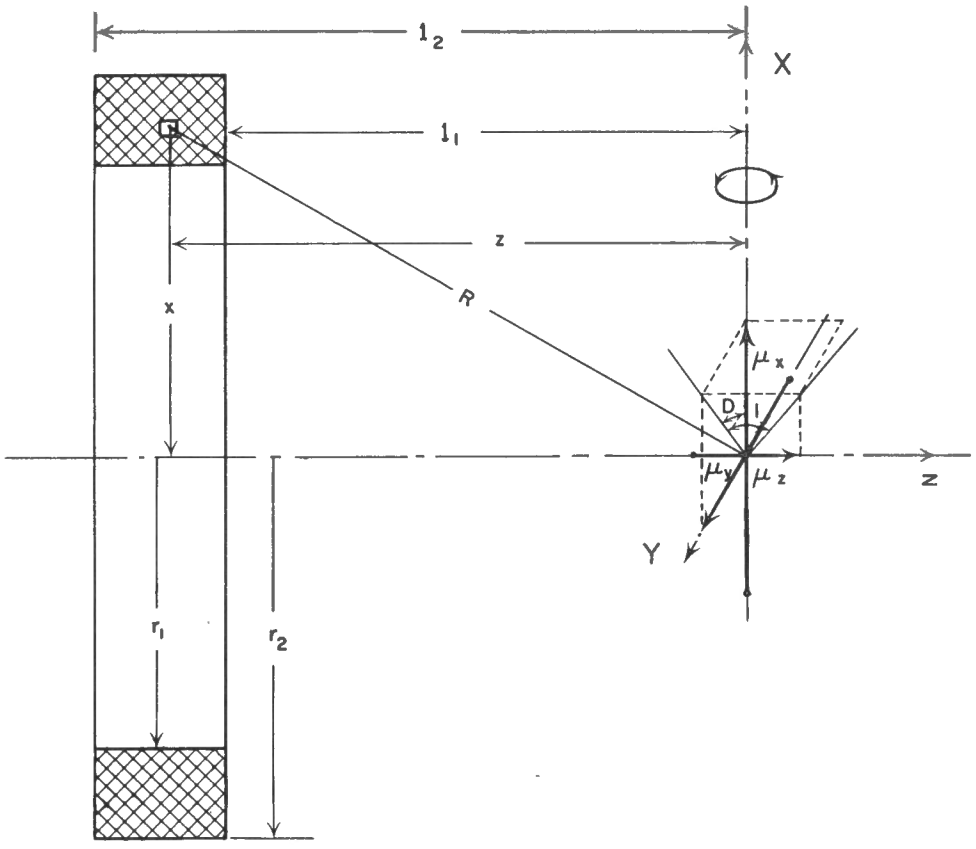

Figure 1. Geometric configuration of pick-up coil and measured dipole

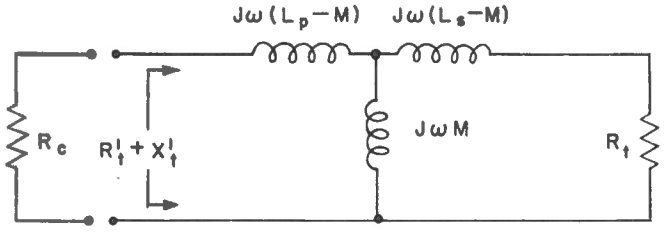

Figure 2. Equivalent circuit of matching transformer

$$\Phi = \frac{2\pi\mu_z\pi}{4a}\int_{r_1}^{r_2}\left[\int_{l_1}^{l_2}\frac{r^2\,dz}{(r^2+z^2)^{3/2}}\right]dr \quad \ldots\ldots\ldots\ldots\ldots\ldots (4)$$

where "a" is the cross-sectional area of the winding wire and $\pi/4$ is the fraction of the winding cross-section occupied by the winding wire if we assume a packing factor of 1. Since

$$\int \frac{dz}{(r^2 + z^2)^{3/2}} = \frac{z}{r^2\,(\sqrt{z^2 + r^2})}$$

and

$$\int \frac{dr}{\sqrt{r^2 + z^2}} = \log_e (r + \sqrt{z^2 + r^2})$$

we may write:

$$\Phi = \frac{\pi^2\mu_z}{2a}\left\{ l_2 \log_e\left(\frac{r_2 + \sqrt{r_2^2 + l_2^2}}{r_1 + \sqrt{r_1^2 + l_2^2}}\right) - l_1 \log_e\left(\frac{r_2 + \sqrt{r_2^2 + l_1^2}}{r_1 + \sqrt{r_1^2 + l_1^2}}\right)\right\} \quad \ldots\ldots\ldots\ldots\ldots\ldots (5)$$

Assuming that the dipole is rotated about the x axis by an angle θ, its component along the z axis becomes

$$\mu_z = \mu_{yz}\cos\theta$$

where μ_{yz} is the component of μ in the yz plane. Setting

$$\theta = 2\pi ft + \epsilon$$

where f is the spinning frequency (cps) and ϵ is the value of θ at the time $t = 0$, we get

$$\frac{d(\mu_z)}{dt} = - \mu_{yz}\, 2\pi f \sin(2\pi f t + \epsilon)$$

and
$$\frac{\partial \Phi}{\partial t} = \frac{- \pi K f \mu_{yz} \sin(2\pi f t + \epsilon)}{a} \quad \ldots\ldots\ldots\ldots\ldots (6)$$

where
$$K = l_2 \log_e \left(\frac{r_2 + \sqrt{r_2^2 + l_2^2}}{r_1 + \sqrt{r_1^2 + l_2^2}} \right) - l_1 \log_e \left(\frac{r_2 + \sqrt{r_2^2 + l_1^2}}{r_1 + \sqrt{r_1^2 + l_1^2}} \right) \quad \ldots\ldots\ldots\ldots\ldots (7)$$

According to Lenz's law an emf E_s will be induced in the coil as a result of the dipole rotation, and the general expression for the instantaneous value of this emf is given by

$$E_s = \frac{-\partial \Phi}{\partial t}\, 10^{-8} \text{ volts.}$$

Thus we may write

$$E_{s(rms)} = \frac{\pi^3 K f \mu_{yz}\, 10^{-8}}{\sqrt{2}\, a} \text{ volts rms} \quad \ldots\ldots\ldots\ldots\ldots (8)$$

where K is in centimetres, a is in square centimetres, f is in cycles per second, and μ_{yz} in cgs units. For a given rock sample of specific shape, μ_{yz} is proportional to the sample's volume and thus E_s is proportional to the product fV, V being the sample's volume.

For the various instruments reported in the literature, values of f ranging between 10 and 525 cps have been used and samples as small as 3.8 cc have been spun. Apart from being as large as possible the sample should have a shape with a relatively high degree of symmetry for reasons dictated both by the dynamics of the system and the necessity of spinning the sample about a minimum of two mutually perpendicular axes to establish

its direction and intensity of magnetization. Cubes and circular cylinders are generally suitable.

Independently of the signal induced by the spinning sample, the thermal agitation of electrons within the coil circuit is also responsible for the appearance of an emf of spurious character at the coil's terminals. The rms value of this emf is given by (Johnson, 1938):

$$E_{n(rms)} = 1.27 \times 10^{-10} \times \left[\Delta f(R_c + R_t)\right]^{1/2} \text{ volts} \quad \ldots\ldots\ldots\ldots\ldots (9)$$

where R_c is the coil's resistance and R_t is the equivalent noise resistance of the first tube of an amplifier of band width Δf to which the coil is connected. In the case where the coil is linked to the amplifier by means of a transformer (as represented schematically in Figure 2) the value of the reflected noise resistance R_t' at the coil may be made negligible compared to R_c. Using the nomenclature of Figure 2 we may write

$$R_t' + X_t' = j\omega (L_p - M) + \frac{j\omega M (j\omega (L_s - M)) + R_t}{j\omega L_s + R_t} = \frac{\omega^2 M^2}{(R_t - j\omega L_s)} + j\omega L_p$$

Since ωL_s may be made small compared to R_t the value of R_t' will be approximately equal to $\omega^2 M^2 / R_t$, which may generally be given a small value compared to R_c. It follows that

$$E_{n(rms)} = 1.27 \times 10^{-10} (R_c \Delta f)^{1/2} \quad \ldots\ldots\ldots\ldots\ldots\ldots\ldots\ldots (10)$$

The resistance R_c of the coil is defined by the relation

$$R_c = \frac{\pi \rho}{4a^2} \int_{l_1}^{l_2} \int_{r_1}^{r_2} 2\pi r \, dr \, dl = \frac{\pi^2 \rho}{4a^2} (l_2 - l_1)(r_2^2 - r_1^2) \quad \ldots . (11)$$

where ρ is the resistivity of the winding material, a is the cross-sectional area of the winding wire, and the other symbols stand for the dimensions represented in Figure 1. Combining equations (8), (10), and (11) we may write

$$E_s/E_n = \frac{\pi^2 f \mu_{yz} \sqrt{2} \; K \; 100}{1.27 \left[\Delta f (l_2 - l_1)(r_2^2 - r_1^2)\right]^{1/2}} \quad \ldots\ldots\ldots\ldots\ldots\ldots (12)$$

Setting $r_2/r_1 = m$, $l_2/r_1 = n$ and $l_1/r_1 = p$ with $m > 1$ and $n > p \geq 0$ we get

$$E_s/E_n = \mu_{yz}\, f\left(\frac{100\,\pi^2\sqrt{2}}{1.27\,(\rho\,\Delta f)^{1/2}}\right)\frac{F(m,\,n,\,p)}{\sqrt{r_1}} \qquad \ldots\ldots\ldots\ldots\ldots\ldots (13)$$

where $F(m, n, p) = \dfrac{K}{\left[(n-p)(m^2-1)\right]^{1/2} r^{3/2}}$

$$= \frac{1}{\left[(n-p)(m^2-1)\right]^{1/2}}\left[n \log_e\left(\frac{m + \sqrt{m^2+n^2}}{1 + \sqrt{1+n^2}}\right) - p \log_e\left(\frac{m + \sqrt{m^2+p^2}}{1 + \sqrt{1+p^2}}\right)\right]$$

$\ldots\ldots\ldots\ldots\ldots\ldots (14)$

From equation (13) it is clear that r_1 should be as small as possible although it seems consistent with the above theory to set its minimum value so that the circle of radius r_1 circumscribes entirely the maximum orthographic projection of the sample in the coil's plane.

The value of $F(m, n, p)$ should normally be obtained for the combination of m, n, and p, yielding:

$$\frac{\partial F}{\partial m} = \frac{\partial F}{\partial n} = \frac{\partial F}{\partial p} = 0$$

As these partial derivatives lead to relatively complex expressions, it is more practical to study the variations of F by computing its values for different combinations of m, n, and p. Such values are plotted against m for different values of p and n in Figures 3a, b and c. An examination of these curves reveals that the maximum value of F is obtained for $p = 0$ (i.e. $l_1 = 0$) with m and n in the vicinity of 3.25 and 2.0 respectively. The condition $p = 0$ implies, however, that the coil's inner radius r_1 must be large enough to accommodate both the sample and its carrier. The minimum value of r_1 is necessarily larger under these conditions than if the sample were spun about an axis distant from the coil by at least the radius of the carrier. Finally, it is noted that the ratio E_s/E_r is multiplied by a factor $\sqrt{2}$ if a second coil is connected in series complementing the first one, provided its parameters are equal to r_1, r_2, $-l_1$ and $-l_2$ respectively, and the two coils are coaxial.

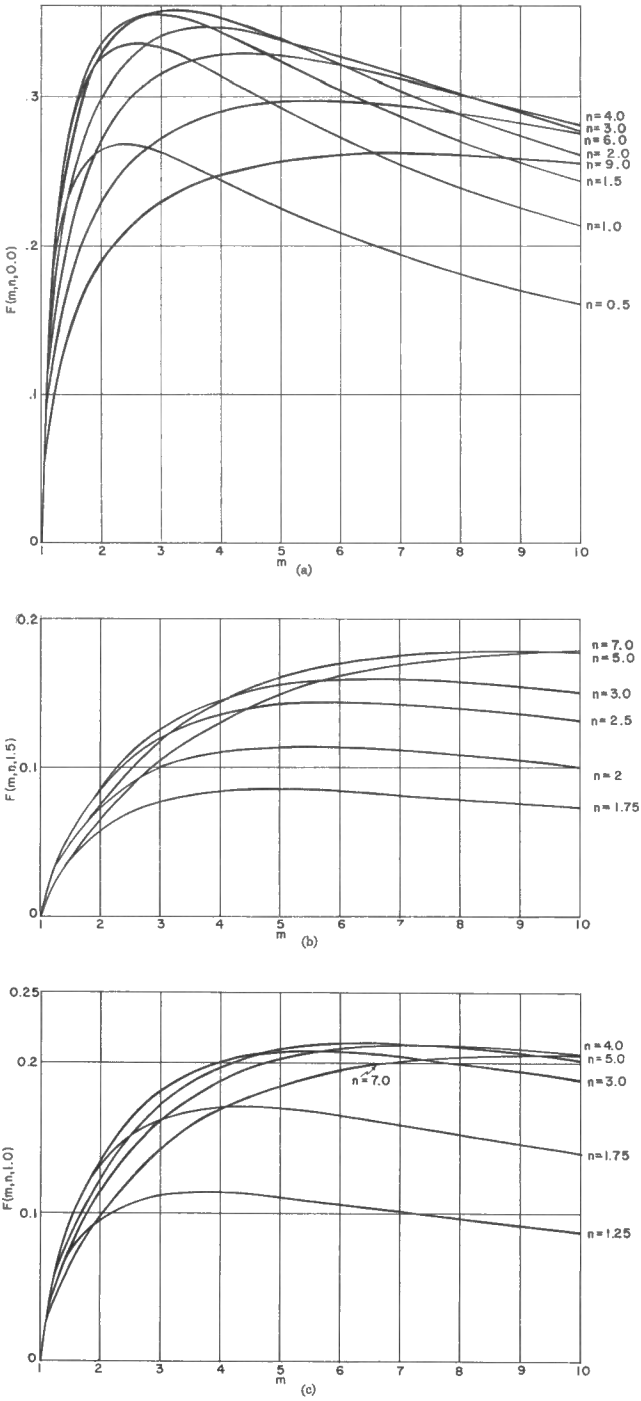

Figure 3. Theoretical variation of (a) F (m, n, 0); (b) F (m, n, 1.5); (c) F (m, n, 1.0)

Superposed to the thermal noise just discussed is another type of voltage noise induced in the coil by ambient field variations or by vibrations of the coil in the same field. Fortunately this type of noise may be practically compensated for by means of a second coil wound in series counter to the pick-up coil, the two coils being mounted coaxially on a common former. Because the component of the ambient field parallel to the coil's axis may have a strong gradient in the plane perpendicular to this axis it is preferable to choose the mean radius of the compensating coil as close as possible to that of the main coil. Compensation of the two coils is reached when their flux linkages are equal, i,e, when

$$\frac{\pi H}{4a}\int_{l_1}^{l_2}\int_{r_1}^{r_2}(\pi r^2)\,dr\,dl = \frac{\pi H}{4a'}\int_{l_1'}^{l_2'}\int_{r_1'}^{r_2'}(\pi r^2)\,dr\,dl$$

$$\text{or}\quad \frac{(r_2^3 - r_1^3)(l_2 - l_1)}{a} = \frac{(r_2'^3 - r_1'^3)(l_2' - l_1')}{a'} \qquad \ldots\ldots\ldots\ldots (15)$$

where the (') refers to the parameters of the compensating coil.

As an emf E_s' is induced in the compensating coil by the spinning sample and as this emf is 180° out of phase with E_s the compensating coil contributes to reduce the efficiency of the pick-up coil. Defining the efficiency of the system as

$$R = \left(\frac{E_s - E_s'}{E_s}\right) 100 = \left(\frac{\frac{K}{a} - \frac{K'}{a'}}{K/a}\right) 100$$

we may write

$$R = \left(1 - \left[\frac{(m^3 - 1)\,F'\sqrt{r_1^3\,(n-p)\,(m'^2 - 1)}}{(m'^3 - 1)\,F\,\sqrt{r_1'^3\,(n'-p')\,(m^2 - 1)}}\right]\right) 100 \qquad \ldots\ldots\ldots\ldots (16)$$

The magnetic moment μ_{yz} in equation (8) refers to the N.R.M. component of the sample in the plane perpendicular to the spinning axis, i.e. the x axis in Figure 1. In order to obtain the total N.R.M. of the sample it is necessary to measure also μ_{yz} and μ_{xy}. This is accomplished by spinning the sample successively with its μ_y and μ_z components parallel to the spinning axis. The total moment μ is defined by

$$\mu = \sqrt{\frac{\mu_{xy}^2 + \mu_{yz}^2 + \mu_{xz}^2}{2}} \quad \text{.............................(17)}$$

The orientation of μ relative to μ_x, μ_y, and μ_z is completely defined by angles D and I, where D is the clockwise angle between μ_x and μ_{xy}, and I is the clockwise angle between μ_{xy} and μ. We may then write

$$\tan(D) = \pm \sqrt{\frac{\mu^2 - \mu_{xz}^2}{\mu^2 - \mu_{yz}^2}} \quad \text{...........................(18a)}$$

and

$$\tan(I) = \pm \sqrt{\frac{\mu^2 - \mu_{xy}}{\mu_{xy}}} \quad \text{...........................(18b)}$$

Equations (18a) and (18b) each lead to four possible solutions, and consequently N.R.M. intensities alone are not sufficient to allow determining the attitude of the magnetic vector with respect to the sample's coordinates system. To eliminate this ambiguity it is necessary to measure at least two of the three angles (μ_x, μ_{xy}), (μ_y, μ_{yz}) and (μ_z, μ_{zx}). These angles, denoted by α, β, and γ respectively, may be made to correspond to the phase angles between the alternating voltages induced in the coil as the sample is spun successively about its μ_z, μ_x, and μ_y axes and a reference alternating voltage of the same frequency whose phase is related to a fixed direction on the sample carrier. Computations of angles D and I from the values of α, β and γ is done by means of the following identities

$$\tan(D) = \tan\alpha = \cot\gamma \cot\beta \quad \text{............................(19a)}$$

and

$$\tan(I) = \tan\beta \sin\alpha = \cot\gamma \cos\alpha = 1/\left(\sqrt{\cot^2\beta + \tan^2\gamma}\right) \text{....(19b)}$$

A corollary to these identities is that

$$\tan\alpha \tan\beta \tan\gamma = 1 \quad \text{..................................(20a)}$$

and

$$\sin \gamma \cos \alpha \geqslant 0 \quad \ldots\ldots\ldots\ldots\ldots\ldots\ldots\ldots\ldots\ldots\ldots\ldots\ldots (20b)$$

so that $D = \alpha$ and $I \sin \beta \geqslant 0$.

DESIGN OF THE GEOLOGICAL SURVEY'S INSTRUMENT

Although the sample is not considered a component of the instrument, its size and shape are of main concern in determining the spinning frequency and the inner radius r_1 of the pick-up coil. The setting of the sample's dimensions was guided in the present design by the fact that the N.R.M. is often found to be inhomogeneously distributed in rocks, even within the restricted dimensions of a hand specimen. To detect such inconsistencies, the practice was adopted in our laboratory of drawing two or more samples from each hand specimen. For this reason a 1-cubic-inch sample was judged satisfactory and the cubic shape was adopted for reasons of symmetry. From an examination of published data listed in Table I it was estimated that no serious difficulties should be encountered in attempting to spin a 1-inch rock cube at the rate of 250 to 300 rps, and the spinning frequency was thus set at 255 rps.

To achieve a spinning frequency of this order the device selected was a conical air turbine such as that described first by Henriot and Huguenard (1925; 1927) and used by Graham (1955) and later by others for spinner magnetometers. The design principles of such a turbine are discussed in detail in a paper by Garman (1933). The dimensions and shape arrived at in the present design are represented in Figure 4. The rotor and stator were machined from a 2-inch lucite rod and the rotor's wall was girdled by an aluminum rim, 1/32 inch thick, to provide a uniform distribution of electrostatic charges picked up as a result of air friction. At 255 revolutions per second the loaded rotor may be maintained within one cycle of its nominal frequency almost indefinitely. The air pressure at the intake of the turbine is controlled manually and adjusted to 22 psig by means of a commercial-type air regulator.

As pointed out originally by Henriot and Huguenard (1927) it is important to mount a conical turbine on a relatively flexible base in order to attenuate the reflection from the stator of vibrations set up in the rotor at high speeds due to minute imperfections in the samples. In the present instrument eight rubber bands stretched in pairs at each corner of the stator's clamp were sufficient to dissipate the above-mentioned vibrations.

Table I

Sample Volumes and Spinning Frequencies
Reported in the Literature

Sample Volume (cc)	Shape	Spinning Frequency (cps)	Volume x Frequency (cc x turns/sec)	Reference
3.38	cyl.	10	33.8	McNish and Johnson (1938)
3.38	cube	20	67.6	Nagata, Akasi and Rikitake (1943)
5.07	cyl.	375	1,910	De Sa and Molyneux (1963)
8.0	cube	20	160	Bruckshaw and Robertson (1948)
50	cyl.	10	500	Johnson, Murphy and Michelson (1949)
12.9	cyl.	282	3,620	Graham (1955)
1.61	cyl.	525	847	Gough (1956)
13.8	cube	23.5	324	Piontkovski (1956)
33.8	cyl.	78	2,640	Stacey (1959)
13.8	cube	40	552	Dianov (1960)
16.4	cube	40	656	Hood (1958)

The reference voltage used to determine angles α, β, and γ is supplied by a germanium phototransistor (type 800, Texas Instruments) whose sensitive element is energized by a light beam reflected from half of the rotor's rim as it spins about its axis. The other half of the rim is coated with dull black paint so as to practically cut off the light impinging on the phototransistor during the first part of the rotation. The resulting square pulse that shows at the output of the phototransistor has necessarily the same frequency as the signal generated in the coil by the spinning of the sample. The phase of the phototransistor signal is fixed by the two reflectivity boundaries on the rotor's rim. In order to measure angles α, β, and γ the cubic sample is spun successively about its μ_z, μ_x, and μ_y axes, while its μ_x, μ_y, and μ_z axes respectively are oriented parallel to the vertical plane containing the two reflectivity boundaries.

In designing the coil system it was necessary to decide first whether the sample should be spun in the median plane of the solenoid (Fig. 5a) or as close as possible to the face of a 'pancake-type' coil (Fig. 5b). With the dimensions of the turbine as given in Figure 4 it was

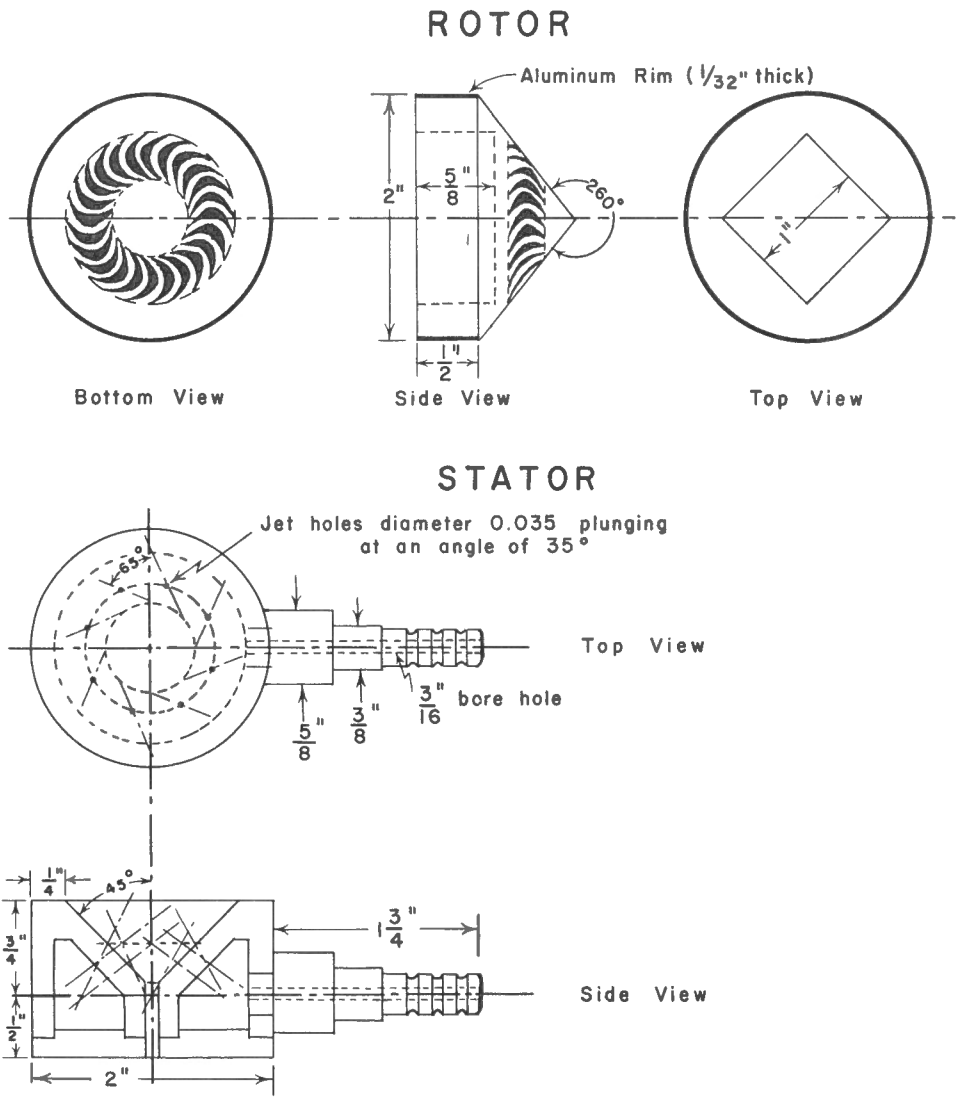

Figure 4. Details of air turbine

estimated that in the first case the minimum value of r_1 is of the order of 2.5 inches whereas the minimum values of r_1 and l_1 in the second case are about 1.0 and 1.5 inches respectively. On the other hand, it may be verified from Figures 3a and 3c that F(m, n, p) may reach a maximum value of 0.358 $\sqrt{2}$ in the first case and of 0.18 in the second case. The principle of the configuration shown in Figure 5a was then adopted.

Although it is important to design the coil with a high E_s/E_n ratio it should be mainly regarded a voltage source, and as such it must be properly matched to its load for maximum power transfer. On the other hand a wide range of voltages are likely to be generated in the coil, depending on the degree of magnetization of the samples to be spun. To operate the amplifying system at a fixed output voltage and to prevent overloading of the preamplifier, an attenuator was introduced at the input of the system. The attenuator used for this purpose (Hewlett-Packard, 132 db) has an image impedance of 50 ohms and, accordingly, the total resistance of the coil system was selected as close as possible to this value.

The total resistance of the actual coil system turned out to be 51 ohms; its other characteristics are given in Figure 6. The calculated values of F(m, n, p) $r_1^{\frac{1}{2}}$, F(m', n', p') $r_1^{\frac{1}{2}}$, and R for the system are 0.214, 0.028, and 61.4 per cent respectively.

The number of turns in the compensating coil was first estimated according to equation (15) and then adjusted experimentally using the following procedure. The system was set up at the centre and along the axis of a 'Helmholtz' coil, 5 feet square, through which a 60 cps current was allowed to flow. The uniform alternating field along the axis of the system was calculated to be 1.46 oersteds. A resulting voltage of 0.6 volt was measured across the pick-up coil and only a fraction of this voltage appeared across the series-connected system. Turns were added in pairs to each section of the compensating coil until the voltage across the system was reduced to a minimum value of 5 millivolts. From these values the system was estimated to be compensated to 99 per cent.

To further shield the pick-up coil from external electromagnetic noise it was enclosed in a box with walls of 1/4-inch-thick aluminum plates. On the other hand the effect of electrostatic charges picked up by the sample during its rotation in air were attenuated by a Faraday shield at the inside of the coil's form. The lucite form was first coated with 'aquadag' and then sprayed with a lacquer. This conducting film was then subdivided in strips parallel to the coil's axis and interconnected at one end, the common junction being grounded to the aluminum box.

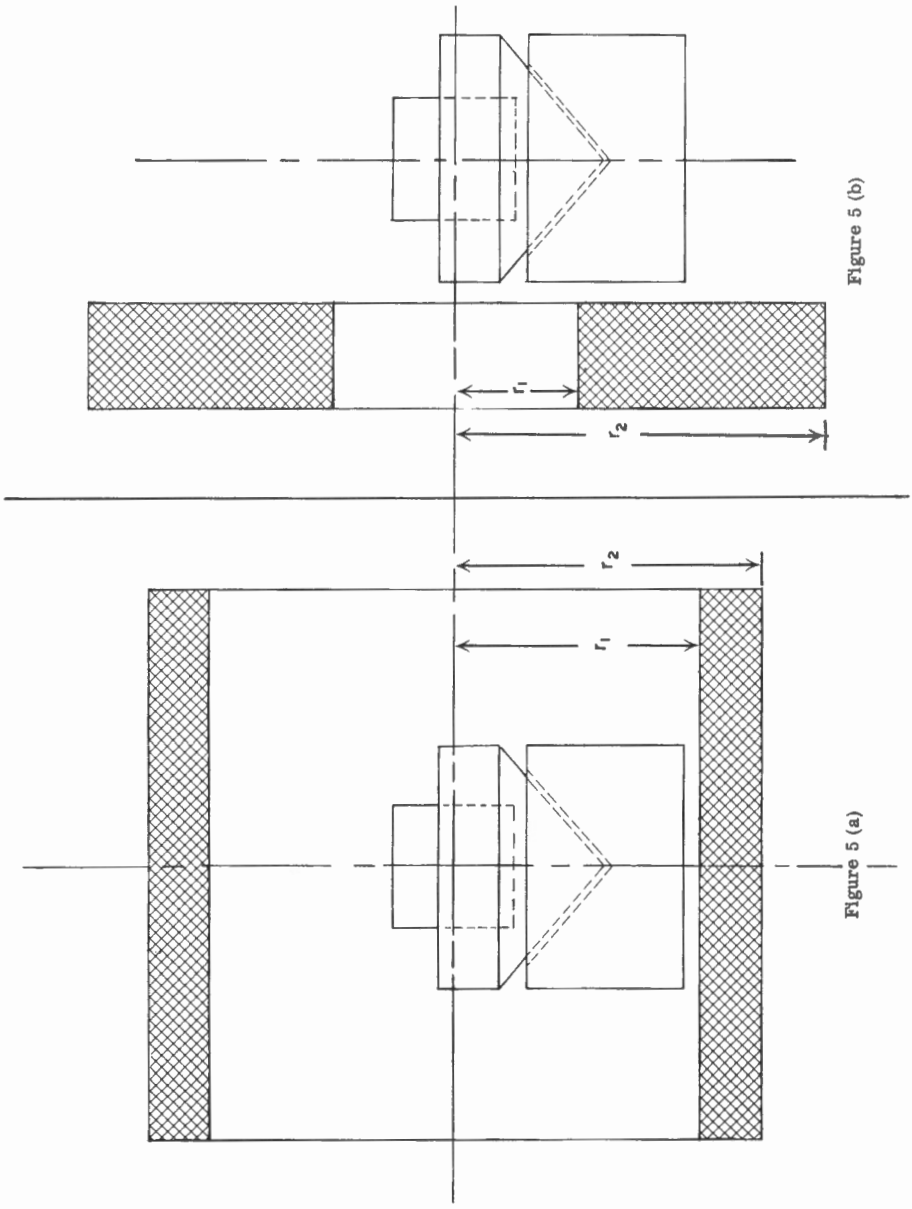

Figure 5 (b)

Figure 5 (a)

Figure 5. Turbine-coil configuration

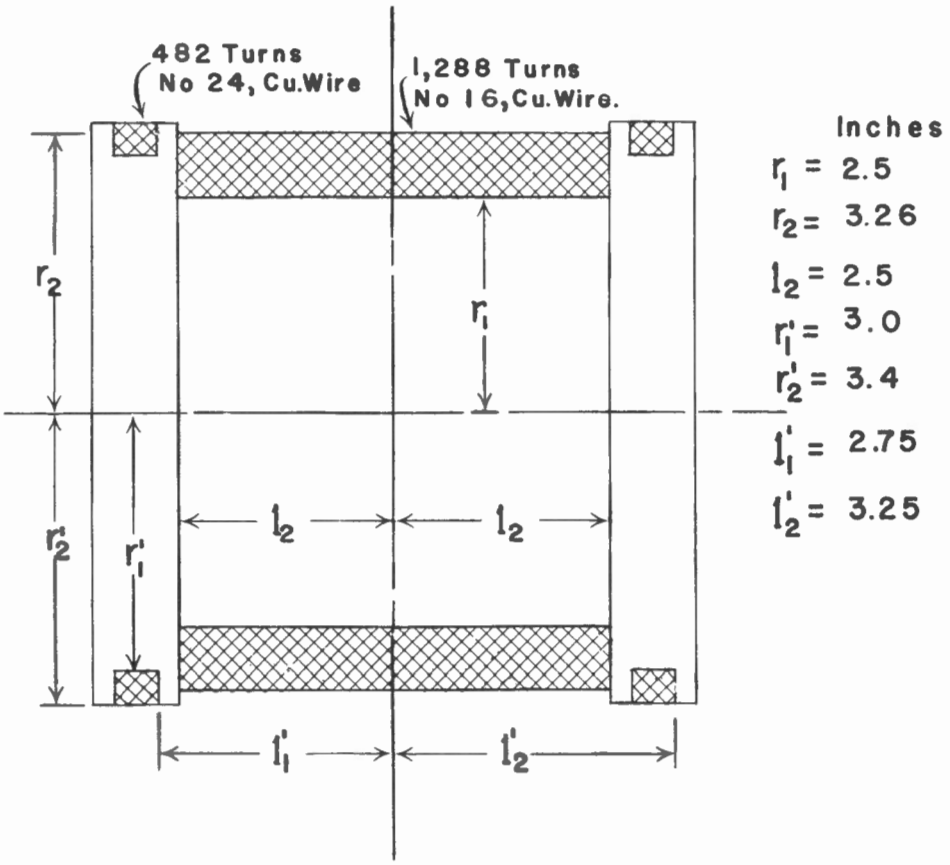

Figure 6. Longitudinal cross-section of coil system

Once the two voltage sources (the phototransistor and the coil signals) were set up, the problem became one of measuring their intensity and their relative phase difference. As mentioned earlier, accurate intensity measurement of the small emf at the terminals of the coil system requires considerable amplification as a preliminary. Referring back to equation (12) it appears obvious also that the amplification should be as selective as possible to provide for a high E_s/E_n ratio, although this feature is also desirable from the point of view of shielding the amplification system from external noise. Another specification of the amplification channels results from the fact that both the phototransistor and coil signals are amplified before their respective phases are compared. It is thus important that the phase-shift response to frequency is identical in both channels, at least within certain limits about the nominal operating frequency of 255 cps. Details of the circuitry through which these conditions were satisfied are shown diagrammatically in Figure 10, which was kindly supplied to the writer by R.H. Ahrens. The principle of its operation is represented schematically in Figure 7. The intensity of the coil's signal is determined from the settings of the attenuator and of the potentiometer, which allow adjusting the output voltage of the amplifier to its nominal value $V_k = 0.4$ volt. Similarly the phase indicator is a fixed output device in that the amplified phototransistor signal is shifted until its phase is exactly 90 degrees from the coil signal. A frequency discriminator is incorporated in the phototransistor signal channel to guide the operator in adjusting the turbine to its nominal speed.

From an examination of Figure 7 we may write

$$V_k = K_1V_1 = K_1V_2 \frac{(500\alpha + 120)}{5,120} = K_1K_2 \frac{(25\alpha + 6)}{256} V_3 =$$

$$K_1K_2 \frac{(25\alpha + 6)}{256} V_4 \times 10^{(\beta/20)} \quad \ldots\ldots\ldots\ldots\ldots\ldots\ldots\ldots \quad (21)$$

where K_1 and K_2 are the gains of the amplifier and preamplifier respectively, α and β are the settings of the potentiometer and attenuator respectively, and V_k .... etc. are the voltages as represented in Figure 7. Since the output impedance of the coil system is very nearly equal to the input impedance of the attenuator, we may write $V_4 = 1/2\ E_s$ and thus

$$V_k = K_1K_2 \frac{(25\alpha + 6)}{256} \frac{E_s}{2} \times \frac{1}{10^{\beta/20}} \quad \ldots\ldots\ldots\ldots\ldots\ldots\ldots\ldots \quad (22)$$

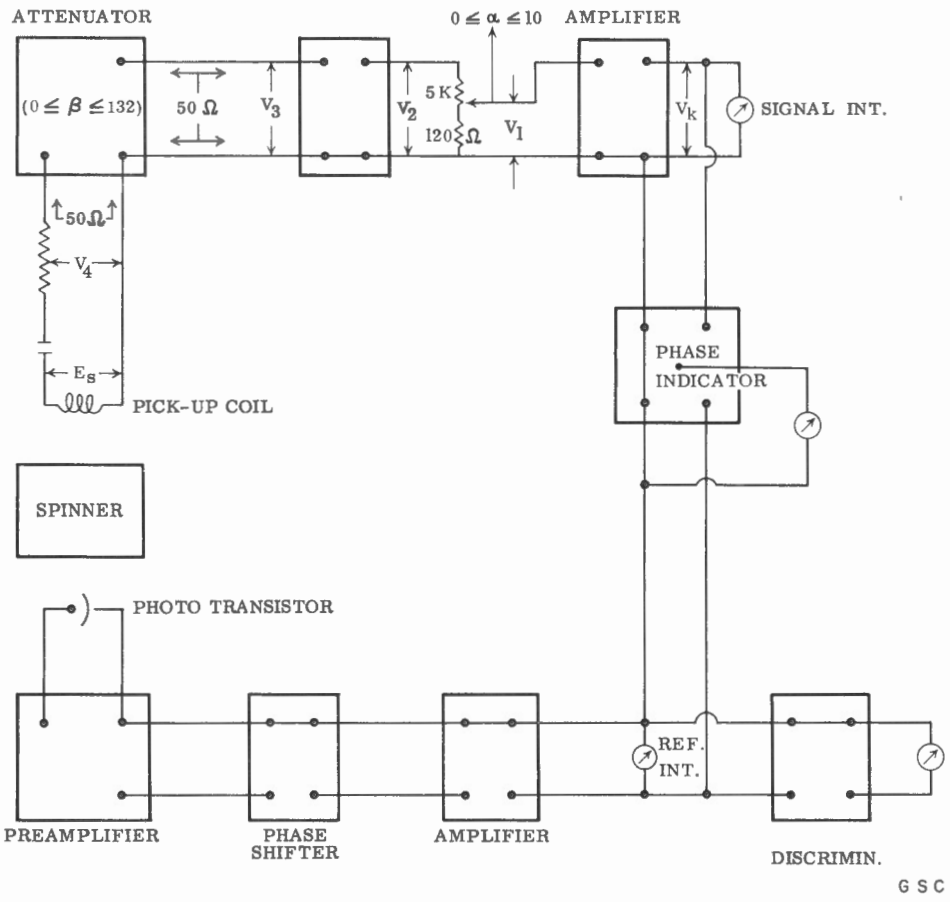

Figure 7. Block diagram of spinner magnetometer electronic circuitry

Combining equations (22) and (8) we get

$$\mu = \frac{M \times 10^{(\beta/20)}}{(25\alpha + 6)} \qquad \text{..................................(23)}$$

or

$$\log_{10}(\mu) = \log_{10}M - \log_{10}(25\alpha + 6) + \frac{\beta}{20} \qquad \text{..................(24)}$$

$$\text{where } M = \frac{4\sqrt{2a}\, V_k\, 256 \times 10^{-8}}{\pi^2 \omega K K_1 K_2}$$

Although M may be calculated from the theoretical or measured values of K_1 and K_2 it may be determined experimentally, as was done in this case. The spinning sample was simulated by a small solenoid connected to a 255-cps voltage generator and set up at the centre of the pick-up coil, coaxially with it. The standardizing solenoid consisted of thirty-four turns of No. 22 enamel-coated copper wire, wound on a 1.25-inch-diameter lucite former. Its magnetic moment μ_c along the axis was evaluated according to the expression

$$\mu_c = \frac{\pi}{4}(1.25 \times 2.54)^2 \frac{34}{10} i,$$

where "i" is the current in amperes allowed to flow in it. The peak value of this current was calculated from the voltage measured with an oscilloscope connected across a 6,000-ohm resistance in series with the solenoid and the voltage source. For a chosen current intensity in the coil, pairs of values were obtained for α and β after the potentiometer and the attenuator had been set so as to adjust the output voltage of the amplifier to its nominal value. As shown in Figure 8 the quantity $\log(1/(25\alpha + 6))$ varies linearly with $\log \mu_c$, and the various straight lines are equally spaced. These facts are in accordance with equation (24), with the expected linearity of the potentiometer and with the predetermined step-up of the attenuator through the series of measurements. For each of the lines in Figure 8 the product $\mu_c(25\alpha + 6)$ was computed and plotted against β on a logarithmic scale in Figure 9. The resulting straight line corresponds to another form of equation (24), namely

$$\log_{10} \mu_c(25\alpha + 6) = \log_{10} M + \beta/20$$

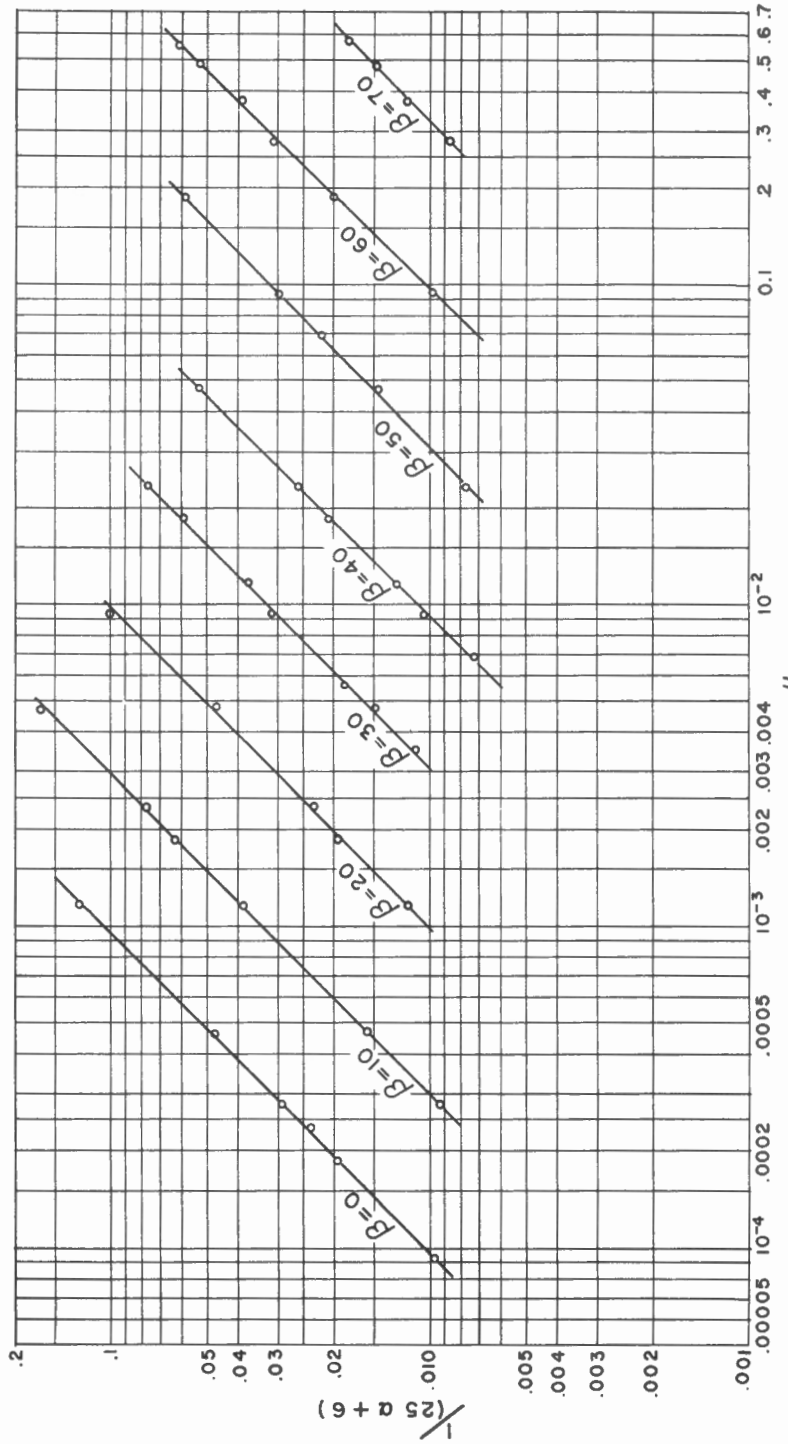

Figure 8. Calibration curves of the spinner magnetometer

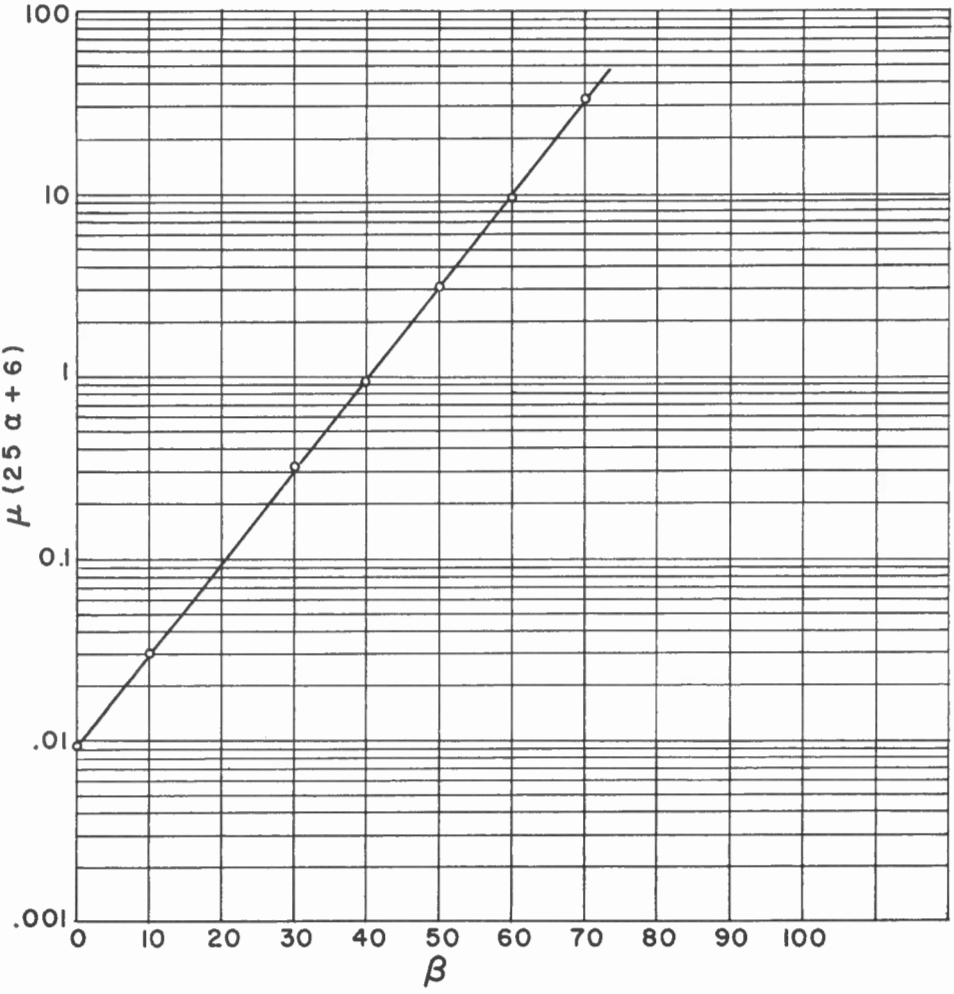

Figure 9. Variation log 10 $(25\alpha + 6)\mu_c$ vs. β

It is easy to see that the value of M in this equation corresponds to the intercept of the line in Figure 9. Using the value of the intercept (9.4×10^{-3} cgs units) we may calculate that the smallest magnetic moment detectable by the instrument is equal to 3.6×10^{-5} cgs units by replacing α and β by 10.0 and 0 respectively in equation (23). Since the sample has a volume of 1 cubic inch, the N.R.M. of a rock having an intensity of magnetization of 2.2×10^{-6} cgs units per cc is thus at the limit of resolution of the instrument.

When the turbine is stationary a voltage of less than 0.01 volt is read at the output of the coil-signal amplifier. Assuming that the gain of the amplifier is linear we may estimate that the background noise in the instrument has an effect corresponding to that of spinning a sample whose magnetization is of the order of 5.5 cgs units per cc. On the other hand if the turbine is spun empty, a voltage of 0.2 volt appears at the output of the amplifier, the settings of α and β being 10.0 and 0 respectively. This corresponds to the effect of spinning a 1-inch-cube sample whose intensity of magnetization would be of the order of 1.1 cgs units per cc.

CONCLUSIONS

The instrument just described is adequate for measuring the N.R.M. of most volcanic and extrusive rocks and it has been used reliably to study certain types of red beds. However, it is not sensitive enough for all rocks that would otherwise be suitable for palaeomagnetic work.

The main advantage of an instrument of this type is that it may be used in laboratories where magnetic-field fluctuations render the operation of an astatic magnetometer impossible. Its drawbacks are common to most high-speed spinner magnetometers: it is relatively slow to operate because of delays imposed by the acceleration and deceleration of the rotor; and it is impossible to spin samples cut from rocks that are above average in density or friability.

BIBLIOGRAPHY

Ahrens, R.H.
1964: The electronic apparatus of the spinner-type magnetometer; Geol. Surv. Can., unpub. MS. on file.

Anderson, L.A.
1961: A remanent magnetometer and magnetic susceptibility bridge; U.S. Geol. Surv., Prof. Paper 424-C, pp. 370-373.

Bancroft, A.M.
1951: The magnetic properties of varved clays; Univ. Birmingham, unpub. M.Sc. thesis.

Blackett, P.M.S.
1952: On a negative experiment relating to magnetism and the earth's rotation; Phil. Trans. Roy. Soc., Ser.A., vol. 245, pp. 309-370.

Bruckshaw, J.McG. and Robertson, E.I.
1948: The measurement of magnetic properties of rocks; J. Sci. Instr., vol. 25, No. 12, pp. 444-446.

Brynjolfsson, A.
1957: Studies of remanent magnetism and viscous magnetism in the basalts of Iceland; Advances in Physics, vol. 6, No. 23, pp. 247-254.

Collinson, D.W. and Creer, K.M.
1960: Methods and techniques in geophysics (Ed. by S.K. Runcorn); Interscience Pub. Inc., New York, N.Y., pp. 190-196.

Daly, L.
1960: Contribution à l'étude de l'anisotropie magnétique dans les roches métamorphiques; Nature de leur aimantation naturelle; Univ. Paris, unpub. thesis.

De Sa, A. and Molyneux, L.
1963: A spinner magnetometer; J. Sci. Instr., vol. 40, pp. 162-165.

Dianov-Klokov, V.I.
1960: An apparatus for measuring small remanent magnetization of rocks; Akad. Nauk., U.S.S.R. Izv. Geof., Ser. No. 1, pp. 142-147.

Garman, W.D.
1933: A study of the high-speed centrifuge; Rev. Sci. Instr., vol. 4, pp. 450-453.

Gough, D.I.
1956: A study of the palaeomagnetism of the Pilansberg dykes; Month. Not., Roy. Astron. Soc., Geophys. Supp., pp. 196-213.

1964: A spinner magnetometer; J. Geophys. Research, vol. 69, No. 12, pp. 2455-2463.

Graham, J.W.
1955: Evidence of polar shift since Triassic time; J. Geoph. Res., vol. 60, No. 3, pp. 329-347.

Graham, K.W.T. and Hales, A.L.
1957: Palaeomagnetic measurements on Karroo dolerites; Advances in Physics, vol. 6, No. 22, pp. 149-161.

Griffiths, D.H.
1955: The remanent magnetism of varved clays from Sweden; Month. Not., Roy. Astron. Soc., Geophys. Supp., vol. 7, No. 3, pp. 103-114.

Henriot, E. and Huguenard, E.
1925: Sur la réalisation de très grandes vitesses de rotation; Comptes Rendus Acad. Sc., Paris, vol. 180, p. 1389.

1927: Les grandes vitesses angulaires obtenues par les rotors sans axe solide; Le Journal de Phys. et le Radium, vol. 8, No. 11, Ser. 6, pp. 433-444.

Hood, P.J.
1958: The design, construction, and calibration of a remanent magnetometer; Univ. Toronto, unpub. M.A. thesis.

Howell, L.G., Martinez, J.D. and Statham, E.H.
1958: Some observations on rock magnetism; Geophysics, vol. 23, No. 2, pp. 285-299.

Johnson, E.A.
1938: The limiting sensitivity of an alternating current method of measuring small magnetic moments; Rev. Sci. Instr., vol. 9, pp. 263-267.

Johnson, E.A., Murphy, T., and Michelson, P.F.
1949: A new high sensitivity remanent magnetometer; Rev. Sci. Instr., vol. 20, No. 6, pp. 429-434.

Kruger, F. and Brasack, F.
1937: Über den natürlichen magnetismus von Kristallen; Annalen der Physik., vol. 30, pp. 113-135.

Larochelle, A.
1962: Palaeomagnetism of the Monteregian Hills, southeastern Quebec; Geol. Surv. Can., Bull. 79, p. 5.

McNish and Johnson, E.A.
1938: Magnetization of unmetamorphosed varves and marine sediments; Terrest. Magnetism, Atm. Electr., vol. 43, No. 4, pp. 393-399.

Morley, L.W.
1952: Correlation of the susceptibility and remanent magnetism with the petrology of rocks from some Precambrian areas in Ontario; Univ. Toronto, unpub. Ph.D. thesis.

Nagata, T.
1961: Rock magnetism; Maruzen Co. Ltd., Tokyo, pp. 58-64.

Nagata, T., Akasi, K., and Rikitake, T.
1943: The remanent magnetism of sedimentary rocks; Bull. Earthq. Res. Inst., Tokyo Imperial Univ., vol. 21, pp. 276-298.

Piontkovski, S.S.
1956: An apparatus for determining the remanent magnetization of rocks; Akad. Nauk. U.S.S.R., Izv., Ser. Geofiz., No. 8, pp. 991-996.

Stacey, F.D.
1959: Spinner magnetometer for thermal demagnetization experiments on rocks; J. Sci. Instr., vol. 36, pp. 355-359.

Vincenz, S.A.A.S.
1952: Remanent magnetism of some igneous rocks of Great Britain and its geophysical significance; Imperial Coll., Univ. London, unpub. Ph.D. thesis.